

RESEARCH ARTICLE

Observable Effects and Peculiarities of the Low-Energy Quantum Gravity

Michael A. Ivanov^{1,*}¹Physics Department, Belarusian State University of Informatics and Radioelectronics, Belarus

Abstract: The existence of a background of ultra-strongly interacting gravitons is a key postulate of the author's low-energy gravity model. Side effects of the model due to photons interacting with this background may be important for cosmology, and their observation would be essential to support the model. The most important such effect is the quantum redshift mechanism, which may constitute an alternative to the generally accepted mechanism associated with the expansion of the universe. The model should have a weakening of the light flux due to a change in the number of photons, which replaces the influence of dark energy. Scattered photons may form a new background that can be detected by deep space missions. Some important predictions of the model are tested using observational data sets of Supernovae Ia (SNe Ia), compact quasars, and Lyman-alpha emitters. The article shows that the linear function $H(z)$ of the model satisfactorily describes the results of measurements of the Hubble parameter. Using a trial function for the weakening parameter, the possibility of a different interpretation of the Hubble tension is illustrated. The increasing angular diameter distance of this model is fitted to a set of 120 measurements of the angular sizes of compact quasars with redshifts of 0.46–2.76 with independent calibration of their linear sizes. Attention is drawn to the possibility of a false interpretation of changes in the measured sizes of Lyman-alpha emitters observed by the James Webb Space Telescope in the redshift range of 3–7 as evolutionary effects in the Lambda Cold Dark Matter (Λ CDM) model, since these changes can be due to the increasing angular diameter distance of this model.

Keywords: graviton background, photon–graviton interaction, redshift quantum mechanism, cosmology

1. Introduction

The discoveries of the last decades in cosmology have an important feature: both dark matter and dark energy [1, 2] are something unknown that has been given a name. Intensive searches are underway for particles that could make up dark matter [3], but it is not even clear where to look for the substance called dark energy. With the increase in the accuracy of measurements and the volume of cosmological surveys, some tensions with the standard cosmological model have appeared, for example, the Hubble tension, forcing one to assume the dynamic nature of dark energy [4, 5]. Attempts to construct a quantum theory of gravity based on Einstein's metric theory have been persistent for decades, but so far without success. Existing testable predictions of such models are few, since the main effects are expected to occur at Planck energies and distances [6]. In the author's model of low-energy quantum gravity, based on the postulate of the existence of a background of superstrongly interacting gravitons, the situation is different [7, 8]. The term "superstrongly interacting gravitons" means that the cross section for interaction between gravitons and any particle is very large. Unlike quantum gravity models based on general relativity, in this model, the interaction of individual gravitons is described by a new constant, D , with the value: $D = 0.795 \cdot 10^{-27} \text{ m}^2/\text{eV}^2$ [7]. For example, the

interaction cross section of a 10-meV graviton and a 1-eV photon in a head-on collision is equal to $\sim 10^{-30} \text{ m}^2$. Cosmic expansion is impossible in this model, as gravity is treated as a screening effect in the background of gravitons. The cosmic distance duality relation of general relativity is not satisfied in the model, as the number of photons is not conserved; some of them are scattered through non-head-on collisions with gravitons. The model is not metric; the gravitational interaction of bodies is described in flat space using forces, with Newton's constant calculated in the model.

The model predicts small effects due to the interaction of photons with this background, which may be of great importance for cosmology. The most important of these is the quantum redshift mechanism, which may become an alternative to the mechanism based on the expansion of the universe. The second effect is due to non-head-on collisions of photons with background gravitons and leads to an additional weakening of the light flux from a distant source, making dark energy unnecessary. The scattered photons should create a new isotropic background, which will be the third effect. Multiple collisions of gravitons with each other should lead to the appearance of a sea of massive virtual gravitons with very low energies, which can pretend to be dark matter particles. The implications of these effects and their differences from the cosmological Λ CDM model are discussed here.

*Corresponding author: Michael A. Ivanov, Physics Department, Belarusian State University of Informatics and Radioelectronics, Belarus. Email: ivanovma@bsuir.by

2. The Hubble Parameter

In this model, the geometric distance r depends on the redshift z as:

$$r(z) = \frac{H_0}{c} \cdot \ln(1+z), \quad (1)$$

where H_0 is the Hubble constant, which can be calculated in this model and has the following theoretical value: $H_0 = 66.875 \text{ km} \cdot \text{s}^{-1} \cdot \text{Mpc}^{-1}$, c is the speed of light (a detailed derivation of the key equations of this paper (e.g., Equations (1), (2), (3), and (6) can be found in references [3] and [13] of the article by Ivanov [8]). The Hubble parameter $H(z)$ in this model without expansion can be defined as [7]:

$$H(z) \equiv \frac{dz}{dr} \cdot c = H_0 \cdot (1+z), \quad (2)$$

which is significantly different from its nonlinear dependence on redshift in Λ CDM. To compare this expression with observations, I have used a full set of 32 observed points $H(z)$ from the paper by Moresco et al. [9] obtained with the cosmic chronometers method and have calculated $\langle H_0 \rangle$ and σ_{H_0} as described in the paper by Ivanov [8]. The obtained result: $\langle H_0 \rangle \pm \sigma_{H_0} = 62.315 \pm 5.84$ has a high C.L. 98.80%, $\chi^2 = 16.718$; this means that the measurement accuracy of $H(z)$ does not allow us to distinguish between this model and Λ CDM. Figure 1 [9] shows the fitting curve with $H_0 = \langle H_0 \rangle$ (solid) and observed points $H(z)$. Moresco et al. [9] estimated the Hubble constant in Λ CDM higher using the same

data set: $\langle H_0 \rangle \pm \sigma_{H_0} = 66.5 \pm 5.4$. The linear function $H(z)$ provides a good fit to other sets of Hubble parameters (see [8] for examples), except for the five-point compilation [8] obtained from the results of the DESI collaboration [10].

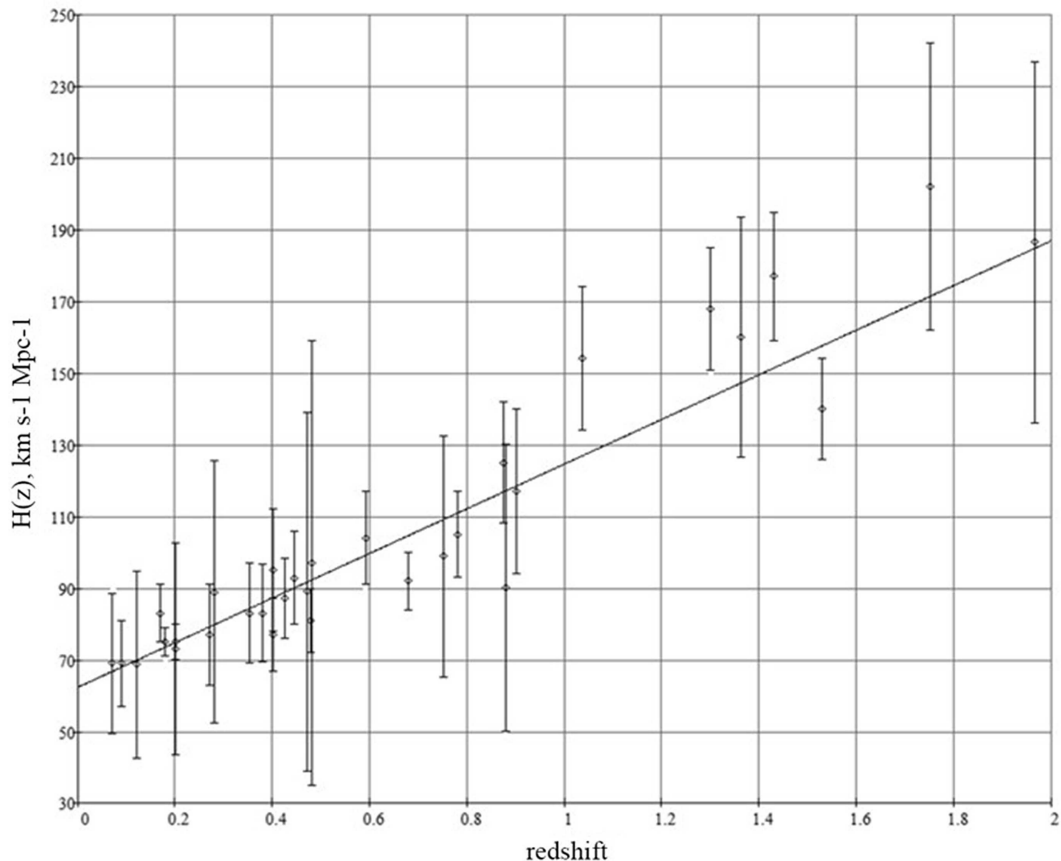
3. Photon Number Losses, the Luminosity Distance, and the Possibility to Re-Interpret the Hubble Tension

In the model, the luminosity distance $D_L(z)$ is equal to:

$$D_L(z) = \frac{c}{H_0} \cdot \ln(1+z) \cdot (1+z)^{(1+b)/2}, \quad (3)$$

where b is the attenuation factor of the luminous flux caused by non-head-on collisions of photons with background gravitons [7, 8]. This factor was calculated for the case of a narrow beam of rays, when a photon after a collision leaves the photon stream registered by a remote observer [8]; $b = 2.137$. For photons with very high energy, $b = 0$ should be. But the exact dependence of b on the photon energy remains an open problem in the model. The dependence of the luminosity distance on the factor b , which can take different values for radiation sources with different spectra, makes the luminosity distance a multi-valued function of the redshift, which is very different from the situation in Λ CDM. This difference in models would be easy to detect by measuring the luminosity distances of distant sources of visible and gamma radiation, for example. Unfortunately, gamma-ray bursts have an unknown absolute luminosity, and they have to be calibrated in Λ CDM using supernovae.

Figure 1
The linear curve fit with $H_0 = \langle H_0 \rangle$ (solid) and 32 observed points $H(z)$



Another open problem is the value of the photon energy at which we will have $b = 2.137$. Since b should increase with decreasing photon energy, this should lead to some increase in b with increasing redshift if $b < 2.137$, that is, to the replacement: $b \rightarrow b(z)$. If $b < 2.137$ in the ultraviolet (UV), visible, and infrared, this should lead to another observable effect – a change in the shape of the spectra of distant sources in these ranges. Spectral lines on the red side of the spectrum should be weakened more than lines on the blue side. It is possible that this putative effect leads to the appearance of small blue galaxies observed by the James Webb Space Telescope (JWST) at redshift $z > 10$ [11, 12].

The ratio $\delta(z)$ of the scattered flux to the remainder that reaches the observer due to photon number losses is also determined by factor b [8]:

$$\delta(z) = (1 + z)^b - 1. \tag{4}$$

The possible formation of a background of visible radiation from these scattered photons may be related to the preliminary detection of a diffuse cosmic optical background by the New Horizons mission [13].

I want to demonstrate here that the possible dependence $b(z)$ allows for a different interpretation of the Hubble tension [14, 15]. If initially this term meant the detected difference between the locally measured value of H_0 and its value obtained by the Planck 2018 team [16] within a Λ CDM scenario (see Figure 2 in the paper by di Valentino et al. [14]), now it is understood somewhat more broadly – as a change in the value of H_0 at different intervals of redshift values [17, 18]. In the paper by

Dainotti et al. [17], the authors use the following phenomenological function $H_0(z)$ to obtain the best fit to the binned values of the Master sample of SNe Ia (Supernovae Ia) data: $H_0(z) = H'_0/(1 + z)^\alpha$, where the parameters H'_0 and α are evaluated.

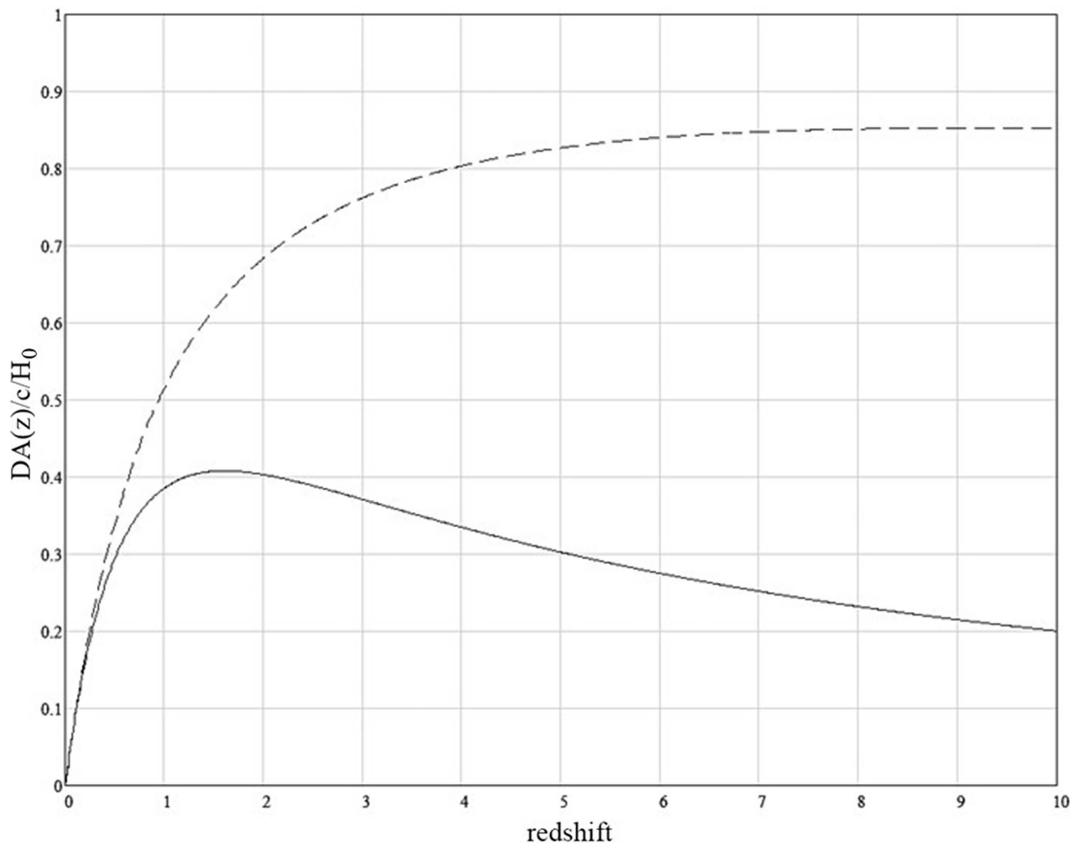
Table 1
The linear functions $b(z)$ and the best fitting values of $\langle H_0 \rangle$ and σ_0 for the Union 2.1 compilation of SNe Ia

$b(z)$	$\langle H_0 \rangle$	σ_0	χ^2	C.L., %
$2.137 + 0.1z$	68.454	6.002	230.535	100
2.137	68.223	6.097	239.635	100
$2.0 + 0.1z$	67.782	6.189	250.159	100
$1.9 + 0.2z$	67.526	6.233	255.600	100
$1.8 + 0.24z$	67.129	6.371	270.000	100
$1.7 + 0.31z$	66.805	6.477	282.010	100

Such a decrease in H_0 with increasing z in my model can be interpreted as an increase in b with increasing z at a constant H_0 . To demonstrate the effect of such a change in b , I chose a linear trial function $b(z) = b_0 + a \cdot z$ and found the best values of H_0 for different values of its parameters b_0 when fitting $D_L(z)$ to the Union 2.1 compilation of SNe Ia [19] corrected for no time dilation. The results are shown in Table 1; we see that the selection of the parameters of the trial function $b(z)$ allows us to reduce the estimate of H_0 . Using Equation (3) with a constant $b = 2.137$ gives for the full data set: $\langle H_0 \rangle \pm \sigma_0 = (68.22 \pm 6.10) \text{ km/s} \cdot$

Figure 2

The angular diameter distance in units of c/H_0 for a flat Universe with concordance cosmology with $\Omega_M = 0.3$ and $w = -1$ (solid) and in this model without expansion (dash)



Mpc, with $\chi^2 = 239.64$, C.L. 100%, while dividing it into two subsets with $z < 0.15$ and $z > 0.15$, we have $\langle H_0 \rangle \pm \sigma_0 = (69.411 \pm 5.402) \text{ km/s} \cdot \text{Mpc}$ for the first subset with $\chi^2 = 124.46$, C.L. 100%, and $\langle H_0 \rangle \pm \sigma_0 = (65.710 \pm 5.391) \text{ km/s} \cdot \text{Mpc}$ for the second one with $\chi^2 = 95.74$, C.L. 100% [8].

4. Model Testability

The cosmic distance duality relation (CDDR):

$$\eta(z) \equiv \frac{D_L(z)}{D_A(z) \cdot (1+z)^2} = 1, \tag{5}$$

where $D_A(z)$ is the angular diameter distance, taking place under the conditions that photon number is conserved, gravity is described by a metric theory, and photons are traveling on unique null geodesics [20]. While the paper by Bassett and Kunz [20] reported small deviations of $\eta(z)$ from 1 caused by excess brightening of Supernovae Ia (SNe Ia) at $z > 0.5$, a recent paper by Kanodia et al. [21] using reconstructed $D_L(z)$ from SNe Ia and $D_A(z)$ from Megamaser data showed that CDDR holds in Λ CDM at $z < 0.04$, and using combining baryon acoustic oscillations (BAO) and SNe Ia data with appropriate choices of calibration parameters, it holds at $0.04 < z < 1.6$. He et al. [22] tested the performance of the CDDR using SNe Ia data (Pantheon data) and the compact radio quasars sample in the redshift range (0.4–2.26). In the paper by Roman et al. [23], the measurement errors of $D_A(z)$ and $H(z)$ in the upcoming SPHEREx survey up to $z = 4.6$ are estimated in the Λ CDM model. The paper by di Valentino et al. [24] describes observational tensions in cosmology, the ways to resolve them, and the key objectives and potential new physics that may be observable in upcoming surveys.

This model differs significantly from the Λ CDM model. It is based on a non-metric gravity model; the number of photons in it changes due to scattering on gravitons – that is, the attenuation of light from distant objects is not associated with dark energy, and space is considered Euclidean, so the angular diameter distance $D_A(z) = r(z)$. There is no expansion of the universe, and therefore, there is no time dilation. If in the Λ CDM model the Hubble constant is a model parameter, then in this model, it can be calculated. The functions $D_A(z)$ of the two models differ greatly, as can be seen in Figure 2. If in Λ CDM $D_A(z)$ has a maximum at $z \approx 1.5$ and then monotonically decreases, in this model, $D_A(z)$ is a growing function, which at $z = 10$ is almost 12 times greater than its analogue in Λ CDM. It may be that this is what leads to the apparent supercompactness of blue galaxies at $z > 10$ [11, 12]. Naturally, CDDR in the form $\eta(z) = 1$ does not take place. The theoretical expression for $\eta(z)$ has the form in this model:

$$\eta(z) \equiv \frac{D_L(z)}{D_A(z) \cdot (1+z)^2} = (1+z)^{(b-3)/2}. \tag{6}$$

This function may be equal to unity for all z , but with the value $b=3$, which is unacceptable in this model. The graphs of Equations (4) and (5) are shown in Figure 3, and to compare the graphs of Equation (5) with the measurements, the $D_L(z)$ values must be corrected for no time dilation.

Using a data set of 120 milliarcsecond compact radio sources in quasars with the redshift range $0.46 < z < 2.76$ and with milliarcsecond angular sizes measured by very-long-baseline interferometry, Cao et al. [25] in the Λ CDM model computed $D_A(z)$ for these sources and evaluated $\langle H_0 \rangle$ to be $67.6 + 7.8 - 7.4 \text{ km s}^{-1} \text{ Mpc}^{-1}$. The size of compact quasars was derived using a

Figure 3
The graphs of Equations (4) (dotted) and (5) with $b = 2.137$ (solid) and $b = 0$ (dashed)

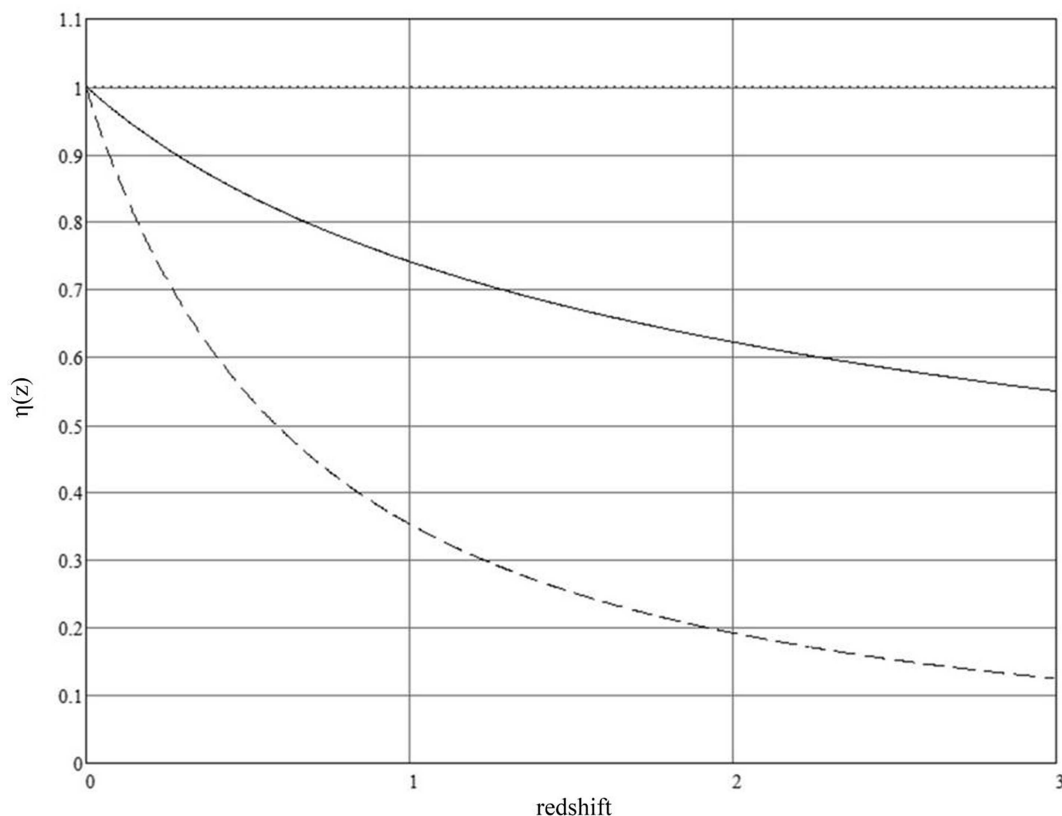
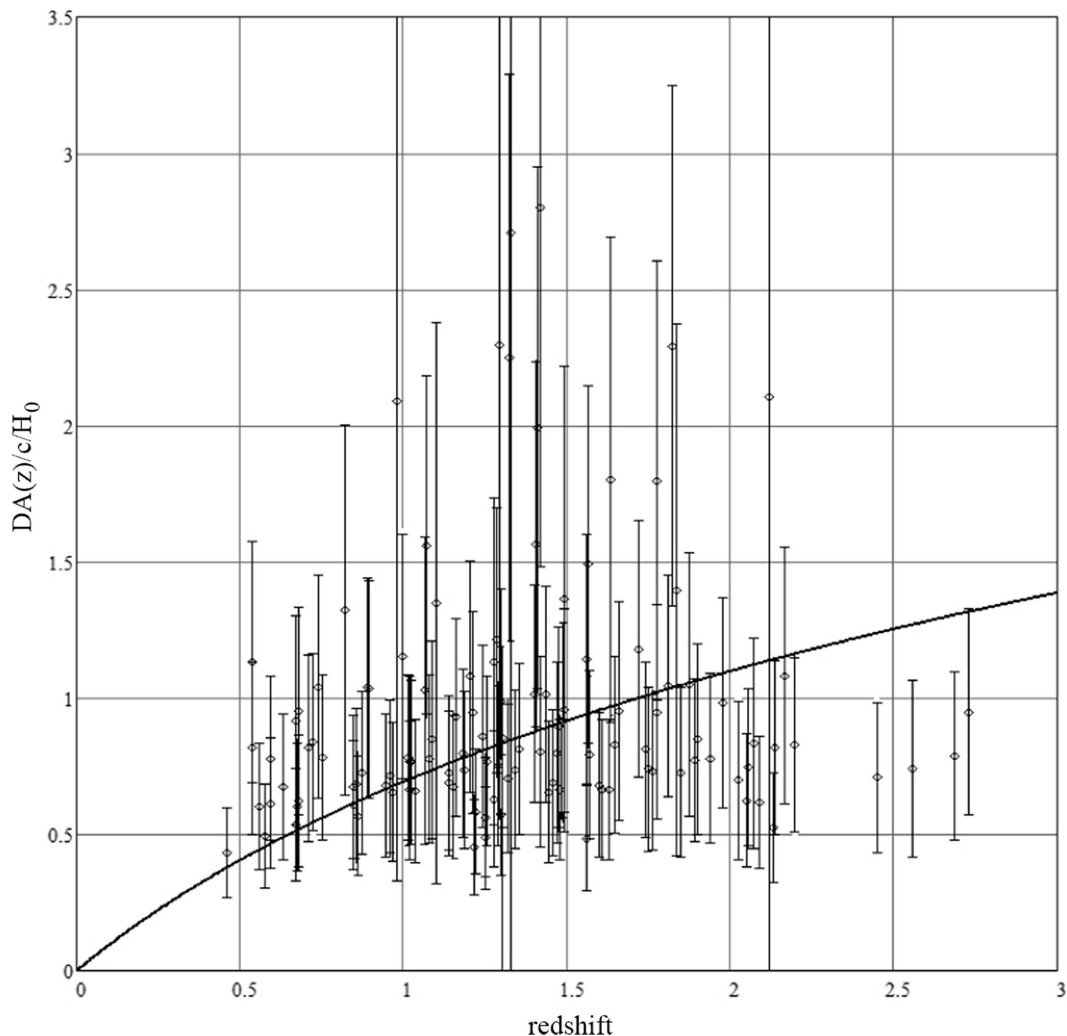


Figure 4
Plot of the theoretical angular diameter distance of this model (solid) and 120 angular diameter distance values calculated from the angular sizes of quasars



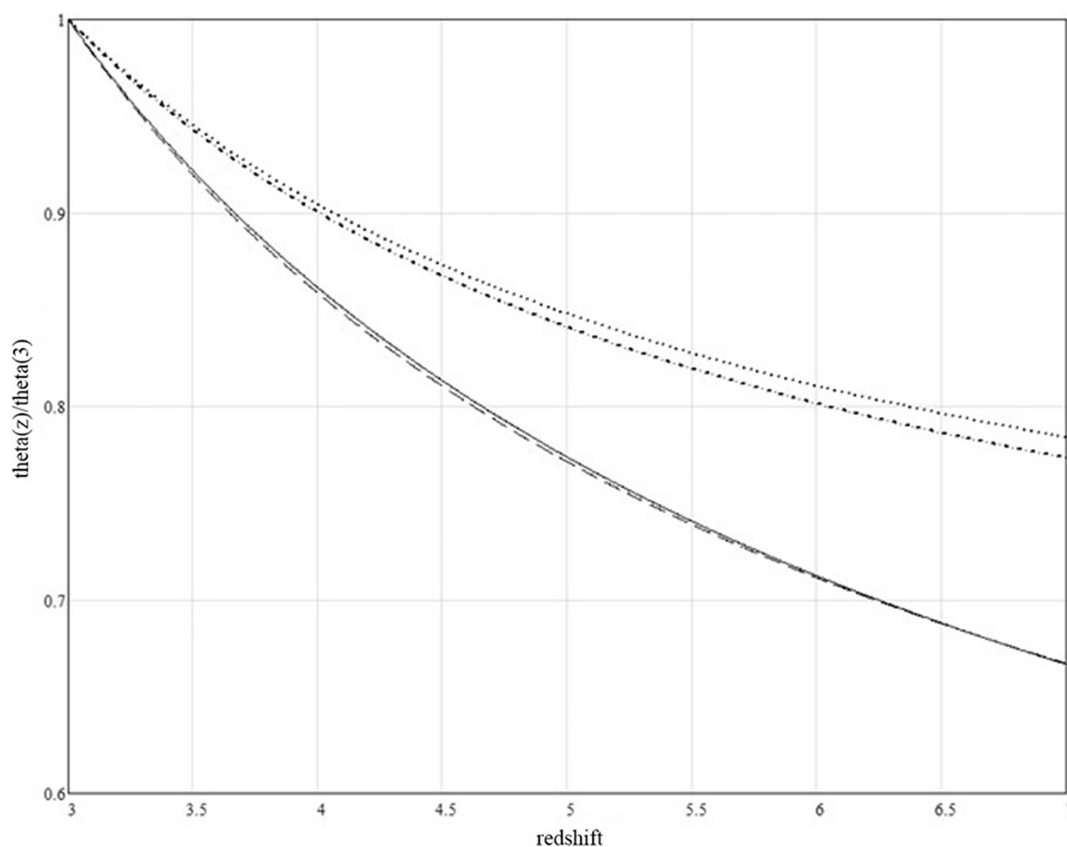
phenomenological model of a source and the observational $H(z)$ data: $l = (11.03 \pm 0.25)$ pc. The obtained values of the angular diameter distance are in agreement with the theoretical curve of the Λ CDM model with $\Omega_{\Lambda} = 0.7$.

In order to use the same data set of the angular sizes of compact quasars to fit the function $D_A(z)$ of this model, it is necessary to estimate the value of l independently of work [25]. To do this, I multiplied the measured values of the angles $\theta(z_i)$ from Table 1 of the article by Cao et al. [25] by the values of the theoretical function $D_A(z)$ for the same z_i . Averaging over all points, I found the following estimate of l in $(c/H_0) \cdot \text{milliarcsec}$ units: $l = (1.187 \pm 0.458)$, or $l = (25.52 \pm 9.84)$ pc with $H_0 = 67.6$ km s $^{-1}$ Mpc $^{-1}$, which is approximately 2.3 times higher than the estimate of the cited work. This difference is due to the different scales of distances in the two models. Using this estimate, I calculated $D_A(z_i)$ using the formula: $D_A(z_i) = \langle l \rangle / \theta(z_i)$ and found the standard deviation $\sigma_{D_A(z_i)}$ for indirect measurements of this quantity. The fitting results are shown in Figure 4 (the angular sizes of quasars are taken from Table 1 of the paper by Cao et al. [25]); in units of (c/H_0) , the theoretical function $D_A(z)$ has no free parameters. The resulting value of χ^2 : $\chi^2 = 98.247$ gives

C.L. **91.75%**. Changing the calibration of the linear size of distant objects increased the angular diameter distance values.

Perhaps measurements of the sizes of Lyman-alpha emitters with images from the JWST [26] are relevant to this topic. In this paper, analyzing a large sample of 876 spectroscopically confirmed Lyman-alpha sources at $3 < z < 7$, the authors found in the Λ CDM model a weak size evolution according to $\propto (1+z)^{-0.91 \pm 0.10}$ and $\propto (1+z)^{-0.93 \pm 0.18}$ in the rest-frame UV and optical ranges. To find the behavior of the measured angular sizes $\theta(z_i)$ of the emitters with changing redshift, I divided each of the two functions $(1+z)^{\langle \beta \rangle}$ by the angular diameter distance $D_A(z)$ in the Λ CDM model with $\Omega_m=0.3$. Since in my model the angular size of distant objects with constant linear size is proportional to $\ln^{-1}(1+z)$, I also found a value of the exponent $\beta_0=-1.143$, at which the function $(1+z)^{\beta_0}/D_A(z)$ in the Λ CDM model well models the function $\ln^{-1}(1+z)$ of this model on the interval $z \in [3, 7]$. The graphs of these functions $\propto \theta(z)$, normalized to unity at $z = 3$, are shown in Figure 5. We see that the graphs of $(1+z)^{\beta_1}/D_A(z)$ and $(1+z)^{\beta_2}/D_A(z)$ go above the graph of $\ln^{-1}(1+z)$ for normalized functions; that is, the size of the Lyman-alpha emitters from the point of view of this

Figure 5
Graphs of the normalized functions $\theta(z)$ of this model for objects of constant linear size (solid) and functions of the form $\theta(z) \propto (1+z)^\beta / D_A(z)$ in the Λ CDM model with $\beta = \beta_0$ (dashed), $\beta = < \beta_1 >$ (dotted) and $\beta = < \beta_2 >$ (dash-dotted)



model rather increases with the growth of z . In units of standard deviations σ_β , the difference between the best value of β_0 for a constant emitter size and the values of β_1 and β_2 found in work by Song et al. [26] is $2.3 \cdot \sigma_{\beta_1}$ and $1.8 \cdot \sigma_{\beta_2}$ in the rest-frame UV and optical ranges, and here, the errors in the absolute sizes of the emitters for $z = 3$ were not taken into account.

An important question is whether this model can be falsified. I believe the most reliable way to do this is to test the quantum nature of the redshift in the model in a ground-based laser experiment. If the model is correct, then such an experiment should detect a weak shifted line after repeatedly passing a laser beam over a distance of several kilometers. With an average photon energy of 1 meV, the photon energy in the red-shifted line should be the same amount less than in the main line. The ratio of the intensities of the red-shifted and main lines should be proportional to the distance traveled by the beam in the high-vacuum tube (more details can be found in reference [13] of the paper by Ivanov [8]).

5. Conclusion

When comparing the theory with the measurement results, it is important to consider the difference in paradigms between this model and the Λ CDM model. The luminosity distance measurements need to be adjusted for the absence of time dilation in this model. The angular diameter distance should be determined using a different calibration for the linear size of distant objects. It is crucial to investigate how the apparent size of an object may be affected by evolution and its relationship to the angular diameter

distance. In this model, the Hubble parameter $H(z)$ is not linked to the history of cosmological expansion; instead, the Hubble constant describes the energy loss of photons as they travel through the graviton background. The small effects discussed in the article have been partially observed but require further examination for a more accurate interpretation. The relationship between the attenuation factor b and photon energy could offer a new perspective on the Hubble tension, but resolving this requires addressing the statistical challenge of multiple non-head-on collisions between photons and gravitons. The possible formation of a background of visible radiation in the model, presumably detected by the New Horizons mission [13], requires additional study by future deep space missions.

Acknowledgment

A pre-publication version of this manuscript was previously posted on the viXra [27].

Ethical Statement

This study does not contain any studies with human or animal subjects performed by the author.

Conflicts of Interest

The author declares that he has no conflicts of interest to this work.

Data Availability Statement

The data that support the findings of this study are openly available at <https://doi.org/10.1007/s41114-022-00040-z>, reference number [9]; <https://doi.org/10.1088/0004-637X/746/1/85>, reference number [19]; <https://doi.org/10.1051/0004-6361/201730551>, reference number [25]; and <https://doi.org/10.3847/1538-4357/ae24e4>, reference number [26].

Author Contribution Statement

Michael A. Ivanov: Conceptualization, Methodology, Validation, Formal analysis, Investigation, Resources, Writing – original draft, Writing – review & editing, Visualization.

References

- [1] Amendola, L., & Tsujikawa, S. (2010). *Dark energy: Theory and observations*. UK: Cambridge University Press. <https://doi.org/10.1017/CBO9780511750823>
- [2] Upadhye, A., Ishak, M., & Steinhardt, P. J. (2005). Dynamical dark energy: Current constraints and forecasts. *Physical Review D*, 72(6), 063501. <https://doi.org/10.1103/PhysRevD.72.063501>
- [3] Sadoulet, B. (2024). Forty years of dark matter searches. *Nuclear Physics B*, 1003, 116509. <https://doi.org/10.1016/j.nuclphysb.2024.116509>
- [4] Zhang, H.-C. (2023). Dynamical dark energy can amplify the expansion rate of the Universe. *Physical Review D*, 107(10), 103529. <https://doi.org/10.1103/PhysRevD.107.103529>
- [5] Wang, J., Yu, H., & Wu, P. (2025). Revisiting cosmic acceleration with DESI BAO. *The European Physical Journal C*, 85(8), 853. <https://doi.org/10.1140/epjc/s10052-025-14593-0>
- [6] Amelino-Camelia, G. (2002). Quantum-gravity phenomenology: Status and prospects. *Modern Physics Letters A*, 17(15n17), 899–922. <https://doi.org/10.1142/S0217732302007612>
- [7] Ivanov, M. A. (2025). Gravity as a screening effect. *Current Physics*, 2(1), e27723348373429. <https://doi.org/10.2174/012723348373429250512104534>
- [8] Ivanov, M. A. (2024). Quantum gravity without quantization. *Current Physics*, 1(1), e27723348344123. <https://doi.org/10.2174/012723348344123241030061731>
- [9] Moresco, M., Amati, L., Amendola, L., Birrer, S., Blakeslee, J. P., Cantiello, M., . . . , & Verde, L. (2022). Unveiling the Universe with emerging cosmological probes. *Living Reviews in Relativity*, 25(1), 6. <https://doi.org/10.1007/s41114-022-00040-z>
- [10] Adame, A. G., Aguilar, J., Ahlen, S., Alam, S., Alexander, D. M., Alvarez, M., . . . , & Zou, H. (2025). DESI 2024 VI: Cosmological constraints from the measurements of baryon acoustic oscillations. *Journal of Cosmology and Astroparticle Physics*, 2025(02), 021. <https://doi.org/10.1088/1475-7516/2025/02/021>
- [11] Ziparo, F., Ferrara, A., Sommovigo, L., & Kohandel, M. (2023). Blue monsters. Why are *JWST* super-early, massive galaxies so blue? *Monthly Notices of the Royal Astronomical Society*, 520(2), 2445–2450. <https://doi.org/10.1093/mnras/stad125>
- [12] Gupta, R. P. (2023). *JWST* early Universe observations and Λ CDM cosmology. *Monthly Notices of the Royal Astronomical Society*, 524(3), 3385–3395. <https://doi.org/10.1093/mnras/stad2032>
- [13] Lauer, T. R., Postman, M., Weaver, H. A., Spencer, J. R., Stern, S. A., Buie, M. W., . . . , & Young, L. A. (2021). New Horizons observations of the cosmic optical background. *The Astrophysical Journal*, 906(2), 77. <https://doi.org/10.3847/1538-4357/abc881>
- [14] di Valentino, E., Mena, O., Pan, S., Visinelli, L., Yang, W., Melchiorri, A., . . . , & Silk, J. (2021). In the realm of the Hubble tension—A review of solutions. *Classical and Quantum Gravity*, 38(15), 153001. <https://doi.org/10.1088/1361-6382/ac086d>
- [15] Riess, A. G., Yuan, W., Macri, L. M., Scolnic, D., Brout, D., Casertano, S., . . . , & Zheng, W. (2022). A comprehensive measurement of the local value of the Hubble constant with 1 km s⁻¹ Mpc⁻¹ uncertainty from the Hubble Space Telescope and the SH0ES team. *The Astrophysical Journal Letters*, 934(1), L7. <https://doi.org/10.3847/2041-8213/ac5c5b>
- [16] Aghanim, N., Akrami, Y., Ashdown, M., Aumont, J., Baccigalupi, C., Ballardini, M., . . . , & Zonca, A. (2020). *Planck* 2018 results: VI. Cosmological parameters. *Astronomy & Astrophysics*, 641, A6. <https://doi.org/10.1051/0004-6361/201833910>
- [17] Dainotti, M. G., de Simone, B., Garg, A., Kohri, K., Bashyal, A., Aich, A., . . . , & Sarkar, H. (2025). A new master supernovae Ia sample and the investigation of the Hubble tension. *Journal of High Energy Astrophysics*, 48, 100405. <https://doi.org/10.1016/j.jheap.2025.100405>
- [18] Hu, J.-P., & Wang, F.-Y. (2023). Hubble tension: The evidence of new physics. *Universe*, 9(2), 94. <https://doi.org/10.3390/universe9020094>
- [19] Suzuki, N., Rubin, D., Lidman, C., Aldering, G., Amanullah, R., Barbary, K., . . . , & Yee, H. K. C. (2012). The *Hubble Space Telescope* cluster supernova survey. V. Improving the dark-energy constraints above $z > 1$ and building an early-type-hosted supernova sample. *The Astrophysical Journal*, 746(1), 85. <https://doi.org/10.1088/0004-637X/746/1/85>
- [20] Bassett, B. A., & Kunz, M. (2004). Cosmic distance-duality as a probe of exotic physics and acceleration. *Physical Review D*, 69(10), 101305. <https://doi.org/10.1103/PhysRevD.69.101305>
- [21] Kanodia, B., Upadhyay, U., & Tiwari, Y. (2026). Revisiting cosmic distance duality with megamasers and DESI DDR2 observations: Model-independent constraints on early-late calibration. *Physical Review D*, 113(2), 023505. <https://doi.org/10.1103/h3f5-7lcr>
- [22] He, Y., Pan, Y., Shi, D.-P., Cao, S., Yu, W.-J., Diao, J.-W., & Qian, W.-L. (2022). Cosmological-model-independent tests of cosmic distance duality relation with Type Ia supernovae and radio quasars. *Chinese Journal of Physics*, 78, 297–307. <https://doi.org/10.1016/j.cjph.2022.06.009>
- [23] Roman, A. M., Ocampo, I., & Nesseris, S. (2026). Forecast constraints on null tests of the Λ CDM model with SPHEREx. *Journal of Cosmology and Astroparticle Physics*, 2026(02), 044. <https://doi.org/10.1088/1475-7516/2026/02/044>
- [24] di Valentino, E., Said, J. L., Riess, A., Pollo, A., Poulin, V., Gómez-Valent, A., . . . , & Davari, Z. (2025). The CosmoVerse White Paper: Addressing observational tensions in cosmology with systematics and fundamental physics. *Physics of the Dark Universe*, 49, 101965. <https://doi.org/10.1016/j.dark.2025.101965>
- [25] Cao, S., Zheng, X., Biesiada, M., Qi, J., Chen, Y., & Zhu, Z.-H. (2017). Ultra-compact structure in intermediate-luminosity

- radio quasars: Building a sample of standard cosmological rulers and improving the dark energy constraints up to $z \sim 3$. *Astronomy & Astrophysics*, 606, A15. <https://doi.org/10.1051/0004-6361/201730551>
- [26] Song, Q., Liu, F. S., Ren, J., Zhao, P., Cui, Q., Li, Y., ..., & Ling, C. (2026). The size evolution and the size-mass relation of Ly α emitters across $3 \leq z < 7$ as observed by JWST. *The Astrophysical Journal*, 997(1), 126. <https://doi.org/10.3847/1538-4357/ae24e4>
- [27] Ivanov, M. A. (2025). *Observable effects and peculiarities of the low-energy quantum gravity*. viXra. <https://vixra.org/abs/2508.0087>

How to Cite: Ivanov, M. A. (2026). Observable Effects and Peculiarities of the Low-Energy Quantum Gravity. *Journal of Optics and Photonics Research*, 3(2), 101–108. <https://doi.org/10.47852/bonviewJOPR62027210>